

# Light- and Hyper-Nuclei Collectivity in Au+Au Collisions at RHIC-STAR

Chengdong Han<sup>1,2,\*</sup> for the STAR Collaboration

<sup>1</sup>Institute of Modern Physics, Chinese Academy of Sciences, Lanzhou 730000, China

<sup>2</sup>School of Nuclear Science and Technology, University of Chinese Academy of Sciences, Beijing 100049, China

**Abstract.** We report the first results on collision energy and particle mass dependence of directed flow  $v_1$  of light- and hyper-nuclei in mid-central Au+Au collisions at center of mass energies per nucleon pair of 3.0, 3.2, 3.5, and 3.9 GeV. All data have been collected by the STAR experiment in the fixed-target mode during the second phase of the RHIC beam energy scan. The mid-rapidity  $v_1$  slope,  $dv_1/dy|_{y=0}$ , of hyper-nuclei shows a similar energy and particle mass dependence to that of light-nuclei. The results suggest that the coalescence mechanism plays a dominant role in the formation of light- and hyper-nuclei.

## 1 Introduction

The two phases of the Beam Energy Scan program at RHIC, BES-I and BES-II, aim to investigate nuclear matter at different temperatures and baryon chemical potentials by colliding gold nuclei at various collision energies. The goal is to study the nature of phase transition to the deconfined phase and search for QCD critical point within the high baryon density region. In astrophysics, the hyperon puzzle in neutron star research refers to the difficulty to reconcile the measured masses of neutron stars with the presence of the hyperons in their interiors. Extracting the strength of the baryon-baryon interaction in a dense nuclear medium experimentally is essential for understanding the inner structure of compact stars.

In the past few decades, the study of baryon-baryon interaction and the properties of QCD matter using light- and hyper-nuclei production in heavy-ion collisions has been a topic of interest. Thermal model [1] and hadronic transport model with coalescence afterburner [2, 3] calculations have predicted abundant production of light- and hyper-nuclei at high baryon density region. This allows for the study of production mechanism of light- and hyper-nuclei in fixed-target  $\sqrt{s_{NN}} = 3.0, 3.2, 3.5$  and 3.9 GeV Au+Au collisions at the STAR experiment. Light-nuclei, in particular, carry information about local baryon density fluctuations at freeze-out, providing insights into the final state nucleon-nucleon ( $N-N$ ) interaction. Hyper-nuclei, on the other hand, offer access to the hyperon-nucleon ( $Y-N$ ) interaction. Collective flow is commonly used to study the properties of matter produced in high energy nuclear collisions, this is primarily due to its sensitivity to the early dynamics of the collision. The first harmonic coefficient of the Fourier expansion of the particle azimuthal distributions in the momentum space is called the directed flow ( $v_1$ ), which is driven by pressure gradients created in such

---

\*e-mail: chdhan@impcas.ac.cn

collisions. Therefore, measurements of light- and hyper-nuclei collectivity make it possible to study  $N - N$  and  $Y - N$  interactions and the Equation of State at high baryon density.

## 2 Experiment and data analysis

The dataset used in this analysis were collected by the STAR experiment at RHIC with the fixed-target setup during 2018-2020 for the center-of-mass energies per nucleon pair of  $\sqrt{s_{NN}} = 3.0, 3.2, 3.5$  and  $3.9$  GeV. A detailed description of the STAR detector system can be found in [4]. The Time Projection Chamber (TPC) [5, 6] is used for charged-particle tracking, while a combination of TPC and Time-of-Flight (TOF) [7] is used for particle identification. The collision centrality is determined by the charged-particle multiplicity distribution measured in TPC within the pseudo-rapidity range  $-2.4 < \eta < 0$  combined with Monte Carlo Glauber models [8, 9]. The event-plane is reconstructed with the Event-Plane-Detector (EPD) within the pseudo-rapidity range  $-5.3 < \eta < -3.3$ . Because of acceptance asymmetry in fixed-target mode collision, three sub-events method was used to determined the event plane resolution.

**Table 1.**  $p_T/A - y$  acceptance windows of light- and hyper-nuclei used for collective flow analysis, where the  $A$  is the atomic mass number.

Particle	$p_T/A$ (GeV/c)	$y$	Particle	$p_T/A$ (GeV/c)	$y$
p	(0.4, 0.8)	(-1.0, 0.0)	t	(0.4, 0.8)	(-1.0, -0.3)
$\Lambda$	(0.4, 0.8)	(-1.0, 0.0)	${}^3\text{He}$	(0.4, 0.8)	(-1.0, 0.0)
d	(0.4, 0.8)	(-1.0, -0.2)	${}^3_{\Lambda}\text{H}$	(0.33, 0.83)	(-1.0, 0.0)
			${}^4\text{He}$	(0.4, 0.8)	(-1.0, -0.4)
			${}^4_{\Lambda}\text{H}$	(0.30, 0.75)	(-1.0, 0.0)

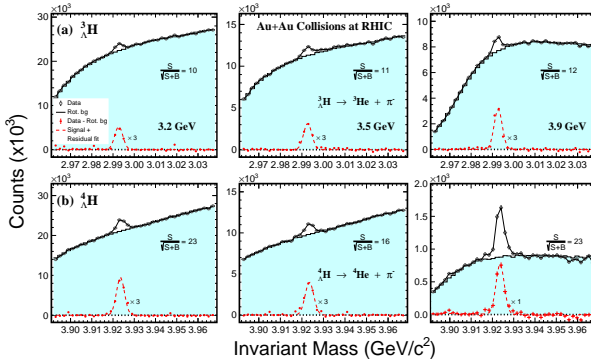


**Figure 1.** Topologically reconstructed (2-body decay)  ${}^3_{\Lambda}\text{H}$  (top panel) and  ${}^4_{\Lambda}\text{H}$  (bottom panel) from 3.2, 3.5 and 3.9 GeV Au+Au collisions. Background subtracted distributions are shown as red symbols. The significances of the mass peaks are also indicated in the figure.

For particle identification, the  $\pi^-$ , p, d, t,  ${}^3\text{He}$ , and  ${}^4\text{He}$  are selected based on the ionization energy loss ( $dE/dx$ ) measured in the TPC as a function of rigidity. For the short-lived hyper-nuclei reconstruction, the secondary decay topology is reconstructed with the KFParticle package based on a Kalman filter method providing a full set of the particle parameters together with their uncertainties. Fig.1 shows the reconstructed invariant mass distributions for  ${}^3_{\Lambda}\text{H}$  and  ${}^4_{\Lambda}\text{H}$  2-body decay using phase space listed in Table 1 for 3.2, 3.5 and 3.9 GeV. Combinatorial backgrounds for hyper-nuclei are constructed by rotating decay daughter particles through a random angle between  $10^\circ$  and  $350^\circ$ . The combinatorial background subtracted distributions are fitted with a Gaussian plus a linear function for hyper-nuclei to extract the signal counts. The signal significance for  ${}^3_{\Lambda}\text{H}$  2-body decay is around 10 and for  ${}^4_{\Lambda}\text{H}$  is around 20.

The  $v_1(y)$  results of  $\Lambda$  hyperon and hyper-nuclei with the event plane method [10], from 5-40% mid-central Au + Au collisions at 3.2, 3.5 and 3.9 GeV, are shown in Fig.2. For comparison, the  $v_1(y)$  of p, d, t,  ${}^3\text{He}$  and  ${}^4\text{He}$  from the same dataset are shown as open markers.

Since the collective flow depends on the  $p_T$  range of particle species, for a meaningful comparison we use same  $p_T/A$  range when comparing different species and it is listed in Table 1. For the  $\Lambda$  hyperon and light-nuclei, we use the third-order polynomial  $v_1(y) = p_0y + p_1y^3$  to fit in order to cover wider rapidity range. The linear terms for the light-nuclei are shown by the dash line in the positive rapidity region. Due to limited statistics for  ${}^3_\Lambda\text{H}$  and  ${}^4_\Lambda\text{H}$ , we used only the first order polynomial  $v_1(y) = p_0y$  to fit. The linear-terms for hyper-nuclei at the mid-rapidity are shown by the red-yellow lines. In all the above cases, the fit is constrained to pass through (0,0) taking advantage of the symmetry. Systematic uncertainties of the measured collective flow mainly come from the event plane resolution and efficiency corrections, identification as well as topological variable cuts. For hyper-nuclei  $v_1$  measurements, the dominant source of systematic uncertainty is from topological cuts. For light-nuclei, the major contributor to systematic uncertainty is arising from the particle misidentification. The total systematic uncertainty is around 13% and 6% for hyper-nuclei and light-nuclei, respectively.

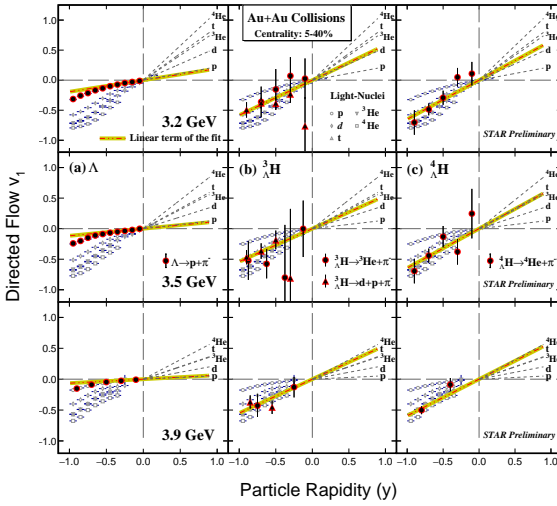


**Figure 2.** Light- and hyper-nuclei directed flow  $v_1$  shown as a function of particle rapidity from 3.2, 3.5 and 3.9 GeV mid-central (5-40%) Au + Au collisions. The rapidity dependence of  $\Lambda$   $v_1$  is shown in left column.  ${}^3_\Lambda\text{H}$ , with both 2-body and 3-body decays, and  ${}^4_\Lambda\text{H}$  rapidity dependence are shown in the middle and right column, respectively. The results of the fit are shown as the red-yellow lines. For comparison, the rapidity dependence for p, d, t,  ${}^3\text{He}$ , and  ${}^4\text{He}$  are shown as open markers and the linear terms of the fitting results for these light-nuclei are displayed as dashed lines in the positive rapidity region.

### 3 Results and Discussion

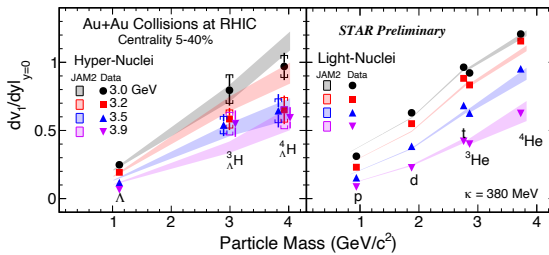


**Figure 3.** Particle mass dependence of the mid-rapidity  $v_1$  slope for hyper-nuclei (left plot) and light-nuclei (right plot) from mid-central 5-40% Au + Au collisions. The results from the 3 GeV data is taken from Ref.[11]. Transport model (JAM [12]) + coalescence results are shown as colored bands.

The results of the mid-rapidity  $v_1$  slope as a function of particle mass for hyper-nuclei and light-nuclei with centrality 5-40% from the  $\sqrt{s_{NN}} = 3.0$  [11], 3.2, 3.5 and 3.9 GeV are shown in Fig. 3. The left panel is for hyper-nuclei mid-rapidity  $v_1$  slope, the right panel is for the light-nuclei mid-rapidity  $v_1$  slope. As we can see, at given energy, for both light- and hyper-nuclei, the mid-rapidity  $v_1$  slopes are scaled with particle mass, implying that coalescence is the dominant process for the light- and hyper-nuclei production. And the feature is also reproduced by hadronic transport model JAM2 ( $\kappa = 380$  MeV) [12] with coalescence afterburner calculations, shown as colored bands.

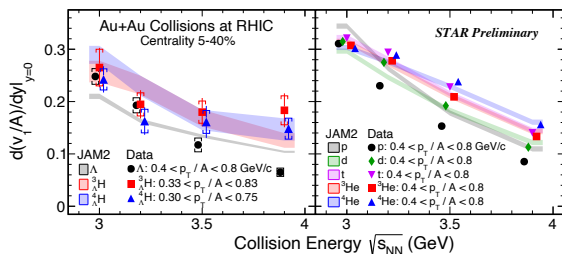


**Figure 4.** Collision energy dependence of the mid-rapidity  $v_1$  slope for hyper-nuclei (left plot) and light-nuclei (right plot) from mid-central 5-40% Au + Au collisions. The results from the 3 GeV data is taken from Ref.[11]. Transport model (JAM [12]) + coalescence results are shown as colored bands.

Figure 4 shows the collision energy dependence of the mass scaled mid-rapidity  $v_1$  slope as a function of collision energy in centrality 5-40% from the  $\sqrt{s_{NN}} = 3.0$  [11], 3.2, 3.5 and 3.9 GeV, for hyper-nuclei on the left panel, light-nuclei on the right panel. From the figure, it can be seen that as the collision energy increases, the mid-rapidity  $v_1$  slope of light- and hyper-nuclei decreases. The hadronic transport model (JAM2) with coalescence afterburner calculations are consistent with observed energy dependence.

## 4 Summary

In these proceedings, we report the collision energy and particle mass dependence of the directed flow  $v_1$  for both light- and hyper-nuclei in  $\sqrt{s_{NN}} = 3.0, 3.2, 3.5$  and  $3.9$  GeV Au + Au collisions measured by the STAR experiment at RHIC. An approximate atomic mass number scaling and energy dependence are observed in the measured  $v_1$  slopes of light- and hyper-nuclei at mid-rapidity. Calculations of hadronic transport JAM model with a coalescence afterburner can qualitatively reproduce the observed dependences for hyper-nuclei as well as light-nuclei collective flow measurements. It suggests that the dominant process in the production mechanism for light clusters is the coalescence process. Moreover, results from a high statistics 2 billion event samples for the 3.0 GeV Au + Au collisions will significantly enhance the precision and help constrain coalescence parameters, as well as constrain  $N - N$  and  $Y - N$  interactions for both light- and hyper-nuclei at the high density region.

## Acknowledgements

This work is supported in part by the National Natural Science Foundation of China under the Grant No. 12305127, the International Partnership Program of the Chinese Academy of Sciences under the Grant No. 016GJHZ2022054FN.

## References

- [1] A. Andronic, P. Braun-Munzinger, J. Stachel, H. Stocker, Phys. Lett. B **697**, 203 (2011)
- [2] J. Steinheimer et al., Phys. Lett. B **714**, 85 (2012)
- [3] J. Aichelin et al., Phys. Rev. C **101**, 044905 (2020)
- [4] K.H. Ackermann et al. (STAR), Nucl. Instrum. Meth. A **499**, 624 (2003)
- [5] M. Anderson et al., Nucl. Instrum. Meth. A **499**, 659 (2003)
- [6] F. Shen et al., Nucl. Instrum. Meth. A **896**, 90 (2018)
- [7] W.J. Llope (STAR), Nucl. Instrum. Meth. A **661**, S110 (2012)
- [8] M.L. Miller et al., Ann. Rev. Nucl. Part. Sci. **57**, 205 (2007)
- [9] R.L. Ray, M. Daugherty, J. Phys. G **35**, 125106 (2008)
- [10] H. Masui, A. Schmah, A.M. Poskanzer, Nucl. Instrum. Meth. A **833**, 181 (2016)
- [11] B. Aboona et al. (STAR), Phys. Rev. Lett. **130**, 212301 (2023)
- [12] Y. Nara, A. Jinno, K. Murase, A. Ohnishi, Phys. Rev. C **106**, 044902 (2022)